Supplementary Material

1 Supplementary Figures

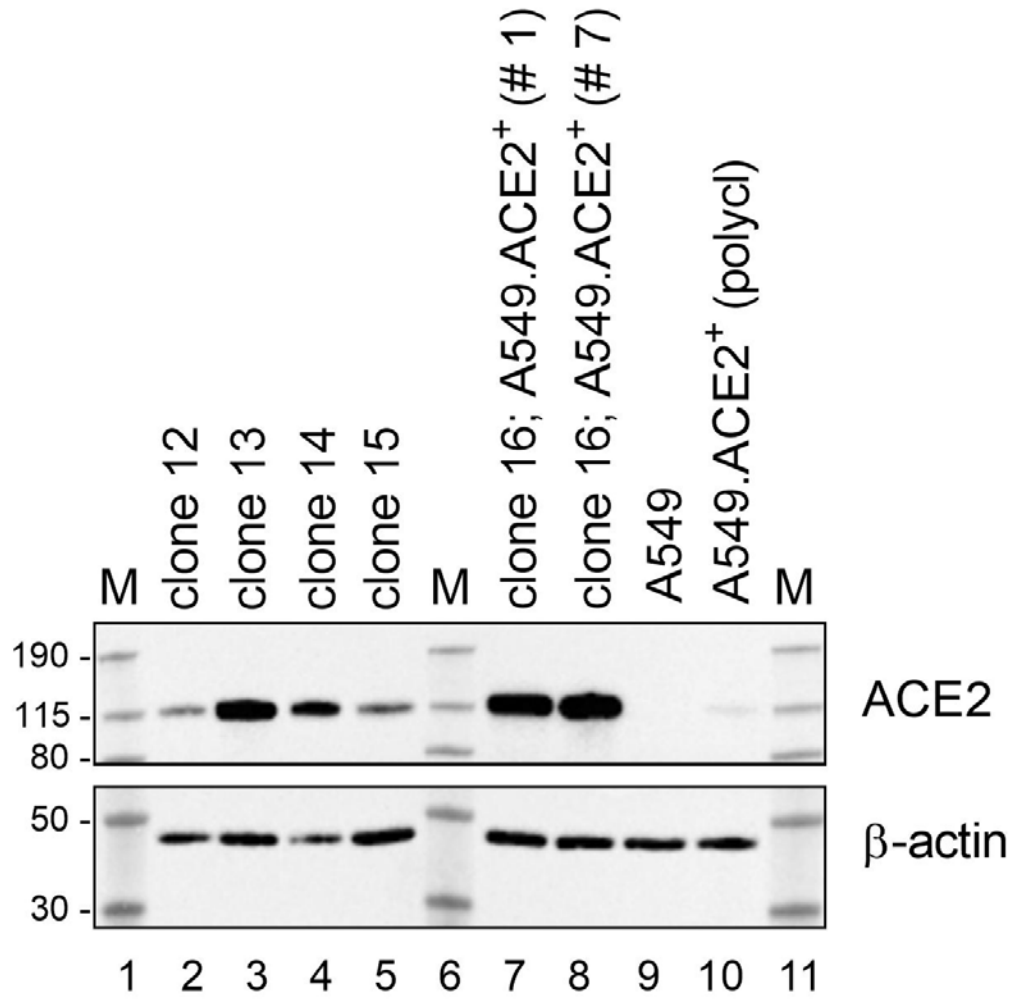

Supplementary Figure 1. Stable expression of ACE2 in transduced A549.ACE2$^+$ cells. Different clones of A549 cells were analysed for ACE2 expression by immunoblotting, with β-actin as loading control. Clone 16 was selected for this study. The stably ACE2 transduced A549 cells (clone 16) were tested at an early (# 1) and later (# 7) passage of the cells (lanes 7 and 8, respectively). The parental A549 cells did not express detectable levels of ACE2 (lane 9). The polyclonal mixture (polycl) of ACE2-transduced A549 cells is also included (lane 10), showing some expression of ACE2. M; molecular marker in kDa.

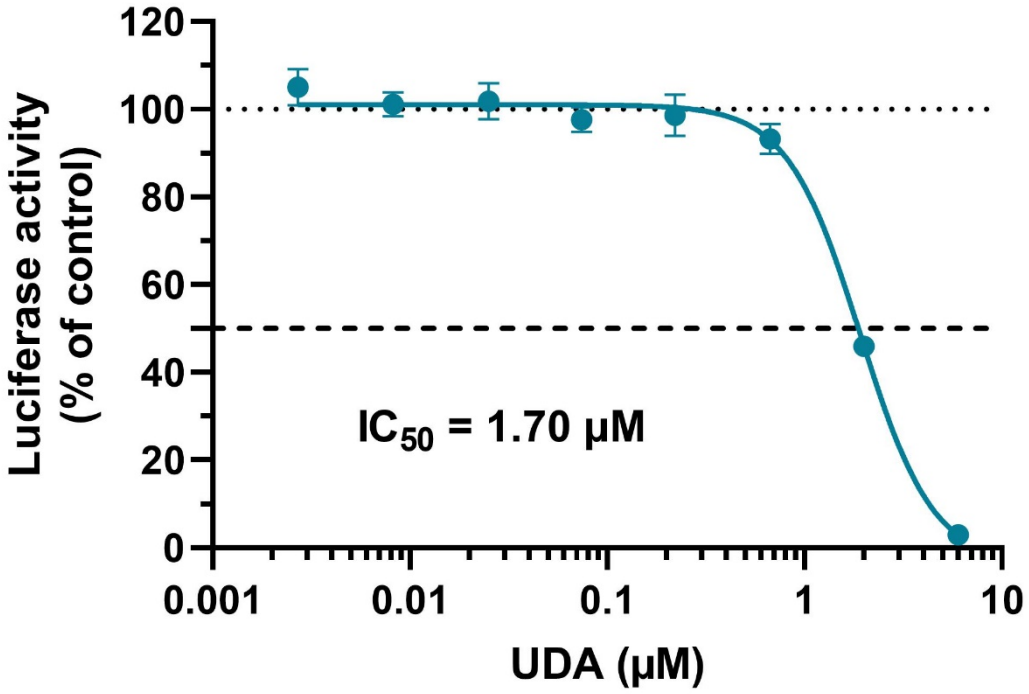

Supplementary Figure 2. Antiviral activity of UDA against pseudotyped Delta SARS-CoV-2. UDA was tested against luciferase-based pseudotyped SARS-CoV-2 (expressing the spike from the Delta VOC) in commercially available A549.ACE2^{+}.TMPRSS2^{+} cells. At 22h after VLP transduction, luciferase activity was measured. Graph represents a concentration-response of UDA from 2 biological replicates in quadruple (mean ± SD; n=8).

A

Ligand/Analyte	k_a ($\times 10^5$ $M^{-1}s^{-1}$)	k_d ($\times 10^{-5}$ s^{-1})	K_D (nM)
Wuhan-Hu-1 spike/UDA (n=8)	3.37 ± 0.22	240.43 ± 13.03	7.37 ± 0.92
Omicron spike/UDA (n=4)	3.49 ± 0.20	364.55 ± 9.25	10.58 ± 0.82
Wuhan-Hu-1 RBD/UDA (n=2)	3.10 ± 0.60	709.50 ± 221.50	22.35 ± 2.85
Wuhan-Hu-1 RBD/R001 (n=3)	19.70 ± 0.87	4.17 ± 0.17	0.020 ± 0.001
Wuhan-Hu-1 RBD/R007 (n=6)	2.93 ± 0.37	16.80 ± 0.89	0.66 ± 0.15
Wuhan-Hu-1 RBD/R007 (n=2)*	4.00 ± 0.77	15.25 ± 1.35	0.39 ± 0.04

B

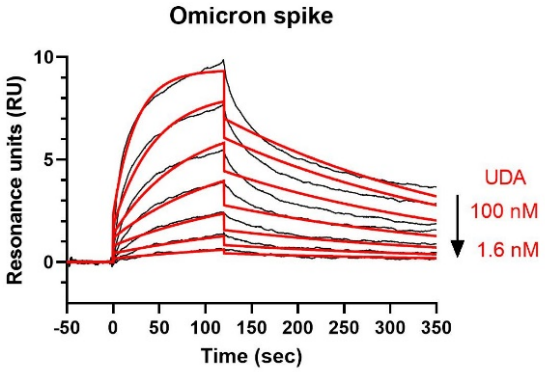

C

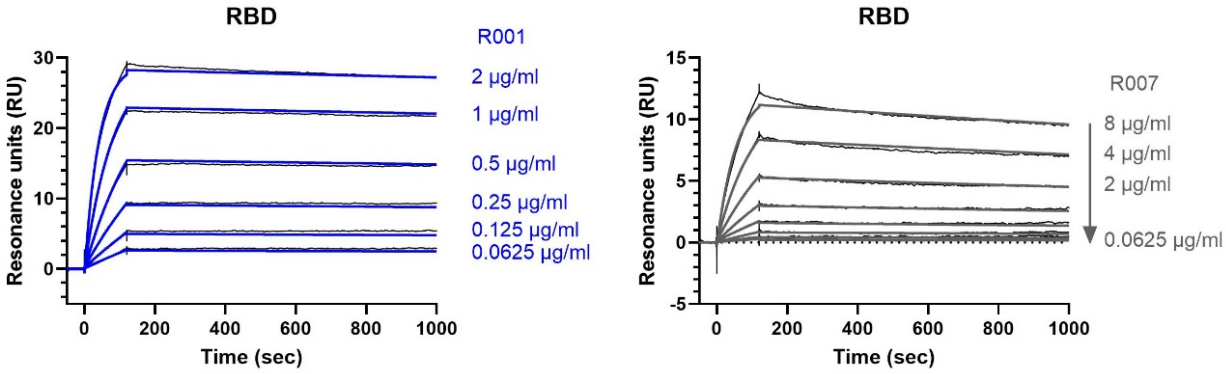

Supplementary Figure 3. Surface plasmon resonance (SPR) analysis of UDA and spike-binding antibodies R001 and R007. (**A**) Summary of the kinetics parameters from different repeat SPR experiments performed in this study. Given are the association rate constant (k_a), the dissociation rate constant (k_d), and the dissociation equilibrium constant (K_D). Values are mean ± SEM. (*) For the

interaction of R007 to RBD, two different sensor chips were used, an NTA chip (n=8) or an CM5 chip (n=2). (**B**) SPR sensorgram showing the binding kinetics for UDA and immobilized monomeric Omicron spike protein (1:2 dilutions of UDA, starting from 100 nM). Data are shown as black lines, and the best fit of the data to a 1:1 binding model is shown in red. (**C**) SPR sensorgrams showing the binding kinetics for spike-binding antibodies and immobilized RBD of Wuhan-Hu-1 spike. Left panel shows sensorgram for the spike-neutralising antibody R001 and right panel that of the non-neutralising spike-binding antibody R007. Data are shown as black lines, and the best fit of the data to a 1:1 binding model is shown in blue or grey, respectively. SPR: surface plasmon resonance; RBD: receptor binding domain; UDA: *Urtica dioica* agglutinin; NTA: nitrilotriacetic acid.

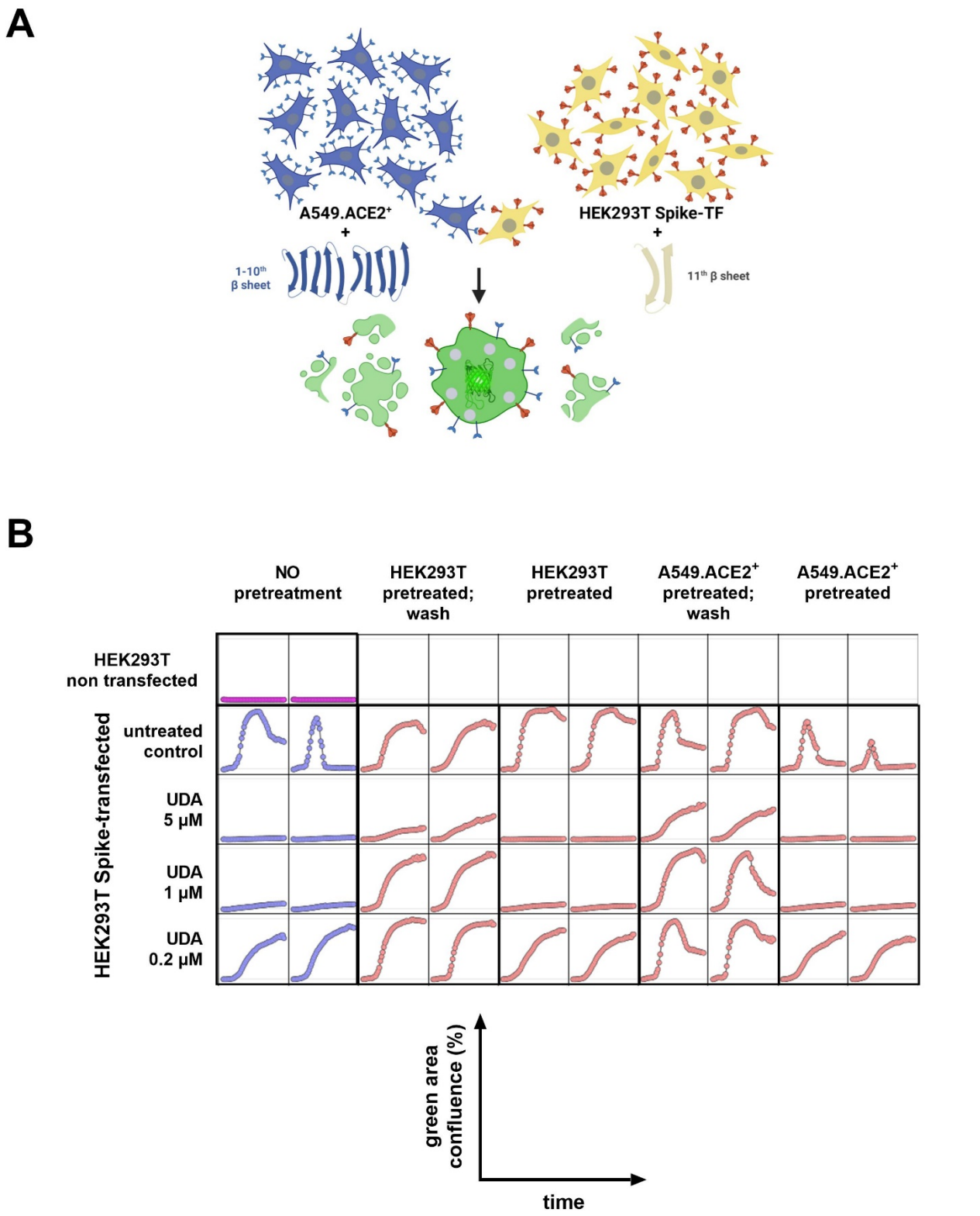

Supplementary Figure 4. UDA prevents cell-cell fusion of A549.ACE2^{+} cells with spike-expressing HEK293T cells. (**A**) A549.ACE2^{+} cells (transfected to express the first 10 betasheets of neongreen) were overlayed with HEK293T cells co-transfected with a plasmid encoding the SARS-CoV-2 spike protein and a plasmid encoding the 11th betasheet of neongreen. Only cell-cell fusion of an A549 cell

with a HEK293T cell will result in the assembly of a functional neongreen protein and give a green fluorescence signal. (**B**) Samples from Figure 5 were analysed for neongreen expression (for specification of the samples, see legend to Figure 5). Each condition was tested in 2 replicate wells (side-by-side columns), and in each well 4 different areas of the cell culture were monitored using an Incucyte live-cell analysis instrument. The increase in neongreen expression over time (17 hours) is plotted as percentage of green area confluence. Each individual plot shows the average signal of the 4 different areas of the cell culture (mean; n=4). Note that because of lysis of the syncytia, the fluorescent protein is diluted in the culture medium, resulting in a drop in the neongreen signal at later time points.

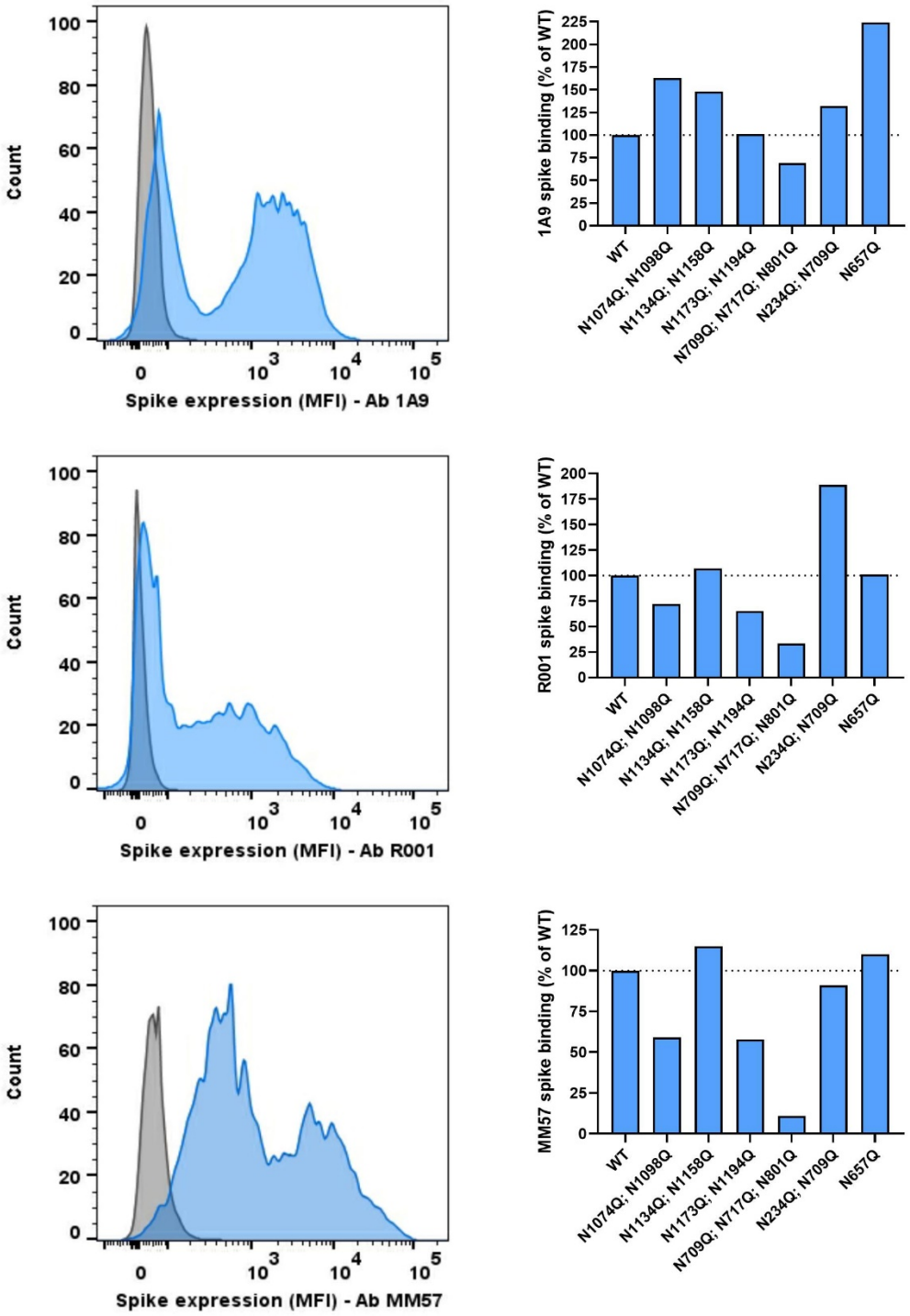

Supplementary Figure 5. Cell surface spike expression of different N-glycosylation mutants. HEK293T cells were transfected with a plasmid encoding the wild-type (WT) SARS-CoV-2 spike protein or an N-glycosylation deletion mutant. At 24h post transfection, cells were collected and stained with three different anti-spike antibodies (as indicated) to determine the cell surface expression of S.

Histogram plots on the left show the mean fluorescence intensity (MFI) of S protein expression for non-transfected (grey) and WT S-transfected (blue) HEK293T cells. Flow cytometric data were collected from approximately 6,000 analyzed cells. The bar graphs on the right show S expression for the different spike mutants as determined by staining with the corresponding anti-spike antibody (as indicated). Bars represent the MFI relative to the WT control.

2 Supplementary Movie

Supplementary movie. A549.ACE2^{+} cells (transfected to express the first 10 betasheets of neongreen) were overlayed with HEK293T cells co-transfected with a plasmid encoding the SARS-CoV-2 spike protein and a plasmid encoding the 11th betasheet of neongreen. Overlay was done in the absence (untreated control; left) or presence of UDA (1 μM; right). Fusion events were visualized using the IncuCyte® S3 Live-Cell Analysis System (Sartorius). Phase contrast and GFP images were taken using a 20x objective lens at 20 minute intervals for a 24 hours period. Image processing was performed using the IncuCyte software.